Biomedical Spectroscopy and Imaging 4 (2015) 269–282
DOI 10.3233/BSI-150116
IOS Press

Solution structures of methyl aldopyranosides revealed by vacuum-ultraviolet electronic circular-dichroism spectroscopy

Koichi Matsuo [a,*], Hirofumi Namatame [a], Masaki Taniguchi [a,b] and Kunihiko Gekko [c,**]
[a] *Hiroshima Synchrotron Radiation Center, Hiroshima University, Higashi-Hiroshima, Japan*
[b] *Department of Physical Science, Graduate School of Science, Hiroshima University, Higashi-Hiroshima, Japan*
[c] *Institute for Sustainable Sciences and Development, Hiroshima University, Higashi-Hiroshima, Japan*

Abstract. Vacuum-ultraviolet (VUV) electronic circular-dichroism (ECD) spectra of methyl β-D-glucopyranoside (methyl β-D-Glc), methyl α- and β-D-galactopyranosides (methyl α- and β-D-Gal), and methyl α- and β-D-xylopyranosides (methyl α- and β-D-Xyl) were measured down to 163 nm in aqueous solution using a synchrotron-radiation VUV-ECD spectrophotometer. Five methyl aldopyranosides exhibited characteristic ECD spectra depending on the gauche (G) and trans (T) conformations of the hydroxymethyl group at C-5 and the α-/β-anomer configurations of the methoxy group at C-1. To elucidate the contributions of these structures to the spectrum, the ECD spectra of three rotamers (GT, GG and TG) of methyl β-D-Glc, methyl α-D-Gal and methyl β-D-Gal were calculated using a time-dependent density functional theory and molecular dynamics simulations. These theoretical spectra were very similar to those observed experimentally, indicating that the GT and GG rotamers show negative and positive ECD around 170 nm, respectively, and that the α- and β-anomers exhibit negative and positive ECD around 160 nm, respectively. These spectral differences between the two rotamers and between the two anomers were attributable to changes in steric configurations, including the intramolecular hydrogen bond around the ring oxygen and the methoxy oxygen, respectively. These relationships were supported by the ECD spectra experimentally observed for methyl α-D-Xyl and methyl β-D-Xyl, demonstrating that the VUV-ECD spectroscopy is a powerful technique for characterizing the structures of saccharides in aqueous solution.

Keywords: Molecular dynamics simulations, saccharide, steric configuration, synchrotron radiation, time-dependent density functional theory

1. Introduction

Saccharides have various biological functions in a living body such as the energy storage (glycogen and starch), the constituents of plant and crustacean/arthropod exoskeletons (cellulose and chitin), the molecular recognition between proteins and cell membranes (mannose and sialic acid), and the protecting biomolecules against damage from cold and dry conditions (trehalose) [11,16,29,30]. The solution

*Corresponding author: Koichi Matsuo, Hiroshima Synchrotron Radiation Center, Hiroshima University, 2-313 Kagamiyama, Higashi-Hiroshima 739-0046, Japan. Tel.: +81 82 424 6293; Fax: +81 82 424 6294; E-mail: pika@hiroshima-u.ac.jp.
**Current address: Hiroshima Synchrotron Radiation Center, Hiroshima University, Higashi-Hiroshima 739-0046, Japan.

structures of saccharides are important for understanding their properties and functions, but they are difficult targets for X-ray crystallography and NMR spectroscopy because saccharides exhibit complicated equilibrium structures in aqueous solution.

Vacuum-ultraviolet (VUV) electronic circular-dichroism (ECD) spectroscopy is a powerful technique for analyzing the structures of saccharides (especially unsubstituted saccharides) in aqueous solution [3,8,12] because they contain hydroxy groups and acetal bonds whose high-energy n–σ^* transitions are detectable only in the VUV region below 190 nm [1,4,17,22,23]. The VUV-ECD spectra of various monosaccharides and their methylated derivatives (methyl aldopyranosides) have been measured down to ∼160 nm in aqueous solution and down to ∼140 nm in the solid state [1,4,17,22,23]. These VUV-ECD spectra are very sensitive to the gauche (G) and trans (T) conformations of the hydroxymethyl group at C-5, the α- and β-anomer configurations of the hydroxy group at C-1, and the axial and equatorial configurations of the hydroxy groups at C-2 and C-4. However, the pairwise relationships between these structures and the ECD of monosaccharides have not been distinctly solved because structural differences of a chromophore might affect not only its own electronic transitions but also those of the other chromophores.

We have recently measured the VUV-ECD spectrum of methyl α-D-glucopyranoside (methyl α-D-Glc) in aqueous solution [18] using a synchrotron-radiation VUV-ECD spectrophotometer [19,25]. The observed spectrum was close to that calculated theoretically with a time-dependent density functional theory (TDDFT) and molecular dynamics (MD) simulations [14,31,32] considering the structural fluctuations and hydration conditions of methyl α-D-Glc in water. These calculations suggested that the ECD spectra of the GT and GG rotamers should be negative and positive around 170 nm, respectively. The accumulation of further experimental and theoretical ECD spectra of monosaccharides could provide more advanced understanding of the complicated equilibrium structures of saccharides in aqueous solution.

In this study we measured the VUV-ECD spectra of methyl β-D-glucopyranoside (methyl β-D-Glc), methyl α-D-galactopyranoside (methyl α-D-Gal) and methyl β-D-galactopyranoside (methyl β-D-Gal), and theoretically calculated their spectra for comparison using the MD and TDDFT methods. These spectra were also compared with the experimentally observed spectra of methyl α-D-xylopyranoside (methyl α-D-Xyl), methyl β-D-xylopyranoside (methyl β-D-Xyl) and three polyols. The contributions of G and T conformations of the hydroxymethyl group and α and β configurations of the anomeric hydroxy group to the VUV-ECD spectrum are discussed in terms of the structural fluctuations and the intramolecular hydrogen bonds of these methyl aldopyranosides.

2. Materials and methods

2.1. Materials

Methyl β-D-Glc, methyl α-D-Gal, methyl β-D-Gal, methyl α-D-Xyl, methyl β-D-Xyl, sorbitol, mannitol and arabitol of high purity (>98%) were purchased from Sigma-Aldrich (St. Louis, MO) and used without further purification. Five solutions of methyl aldopyranosides were freshly prepared by dissolving them in heavy water at a concentration of 10.0 (w/v%), and three polyols were dissolved in distilled water at a concentration of 20.0 (w/v%). The concentrations of these solutes were determined by a dry-weight method. The obtained sample solutions were incubated at room temperature for a day before measuring their VUV-ECD spectra.

2.2. VUV-ECD measurements

The VUV-ECD spectra of five methyl aldopyranosides and three polyols were measured in the wavelength region from 210 to ∼163 nm at 25°C using a VUV-ECD spectrophotometer at Hiroshima Synchrotron Radiation Center. The details of the optical devices of this spectrophotometer are available elsewhere [19,25]. The VUV-ECD spectra were measured using an assembled-type optical cell with CaF_2 windows [19]. The path length of the cell was adjusted with a Teflon spacer to 10 μm for the measurements down to 175 nm, and no spacer was used for the measurements below 175 nm to reduce the light absorption of the solvent. The spectra obtained without the spacer were calibrated by normalizing the ellipticities to the spectra measured using a 10-μm spacer in the overlapping wavelength region from 210 to 175 nm. Each spectrum was recorded with a 1.0-mm slit width, an 8-s time constant, an 8-nm/min scan speed, and using four accumulations. The molar ellipticity, $[\theta]$, was calculated using the molecular weight of the solute. The ellipticity was reproducible within an error of ±5%, which was mainly attributable to noise and to inaccuracy in the path length of the optical cell.

2.3. Initial structures

The initial structures of GT rotamers of methyl β-D-Glc, methyl α-D-Gal and methyl β-D-Gal were obtained from their crystal structures [26] (Fig. 1). The initial structures of the GG and TG rotamers of methyl β-D-Glc were constructed by exchanging the positions of the hydroxy group and the hydrogen atom at C-6 in the GT crystal structures (Fig. 1). The initial structures of the GG and TG rotamers of methyl α-D-Gal and methyl β-D-Gal were obtained in the same manner.

2.4. MD simulations

MD simulations of methyl β-D-Glc, methyl α-D-Gal and methyl β-D-Gal in solution were carried out as described previously [18]. All initial structures of the GG, GT and TG rotamers were immersed in a periodic box (with approximate dimensions of 28 Å × 28 Å × 25 Å) with about 650 TIP3P water molecules in AMBER 11 software [5,13]. Energy minimizations and simulations of each initial structure were performed under the AMBER/GLYCAM force field [15] as follows. Initial steepest-descent energy minimization (1000 cycles) was carried out on the system to relax any steric hindrances artificially produced by the initialization procedure. The energy minimization was carried out for 200 ps

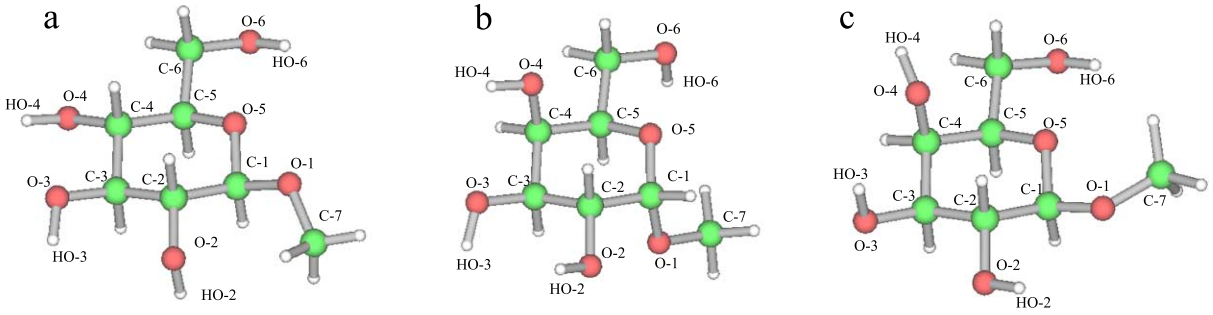

Fig. 1. Crystal structures of the GT rotamers of (a) methyl β-D-Glc, (b) methyl α-D-Gal and (c) methyl β-D-Gal. Oxygen, hydrogen and carbon atoms are colored red, white and green, respectively. The dihedral angles of O-5–C-5–C-6–O-6 involving the hydroxymethyl group at C-5 are 60°, −60° and 180° for the GT, GG and TG rotamers, respectively. (The colors are visible in the online version of the article; http://dx.doi.org/10.3233/BSI-150116.)

while increasing the temperature of the system from 0 to 298 K. After heating, the obtained system was simulated for 20 ns at 298 K and 1 atm using the Berendsen coupling algorithm [2] with $\tau = 1.0$ ps. The particle-mesh Ewald method [7] was used to calculate the electrostatic interactions, with a cutoff of 8 Å for the direct-space sum. We also used a cutoff of 8 Å for the van der Waals interactions. The SHAKE algorithm with an integration time step of 1.0 fs [28] was applied to constrain all of the bonds involving hydrogen. The dihedral angle of O-5–C-5–C-6–O-6 switched among the GG, GT and TG conformations during the 20-ns simulations. Therefore, we slightly restricted the movements of the atoms (O-5, C-5, C-6, O-6) using "RESTRAINTMASK" keyword to enhance the barrier for the switching until the dihedral angle converged to any of the three conformations.

2.5. Calculation of ECD spectra

ECD is induced by the interaction between electric and magnetic dipole transition moments of chromophores and the electromagnetic field of a light wave. As for the relationship between the absorption and the dipole strength, ECD is related to the rotational strength, R, which is theoretically defined by [3,9,10]

$$R_{0a} = \mathrm{Im}\left\{\langle\Psi_0|\hat{\boldsymbol{\mu}}|\Psi_a\rangle \cdot \langle\Psi_a|\hat{\mathbf{m}}|\Psi_0\rangle\right\}, \tag{1}$$

where R_{0a} is the rotational strength of the electric transition from the '0' to the 'a' state, $\hat{\boldsymbol{\mu}}$ and $\hat{\mathbf{m}}$ are the electric and magnetic dipole moments, respectively, and Im{} indicates the imaginary part of a complex number. The rotational strength is expressed in cgs units (erg cm^3), which are conveniently transformed into Debye–Bohr magnetons (DBM) according to 1 DBM $= 0.9273 \times 10^{-38}$ erg cm^3 $= 0.9273 \times 10^{-51}$ J m^3.

The final ECD spectrum can be calculated using the following equations:

$$R_i = 1.23 \times 10^{-42} \frac{[\theta]_i \Delta\sigma}{\sigma_i}, \tag{2}$$

$$[\theta](\sigma) = \sum_i [\theta]_i \exp\left[-\left(\frac{\sigma - \sigma_i}{\Delta\sigma}\right)^2\right], \tag{3}$$

where $[\theta]$ is the molar ellipticity, σ_i is the energy of the ith transition and $\Delta\sigma$ is the half bandwidth of a spectrum calculated assuming a Gaussian distribution. The rotational strength, R_i, was calculated with a TDDFT method at the CAM-B3LYP/6-311++G** level [27,33] and with a polarized continuum model [20] to account for the effects of the solvent in the Gaussian 09 program. From the obtained rotational strength, ECD spectra were calculated using Eqs (2) and (3) with a $\Delta\sigma$ value of 0.40 eV. All of the theoretical spectra were calculated in the energy scale and converted to the wavelength scale. Thirty excited states were considered for the TDDFT calculations.

3. Results and discussion

3.1. VUV-ECD spectra of methyl aldopyranosides

Figure 2 shows the VUV-ECD spectra of methyl β-D-Glc, methyl α-D-Gal, methyl β-D-Gal, methyl α-D-Xyl and methyl β-D-Xyl in heavy water down to 163 nm. The spectrum of methyl α-D-Glc measured in a previous study [18] is also shown in Fig. 2(a) for comparison. Methyl β-D-Glc exhibited a very

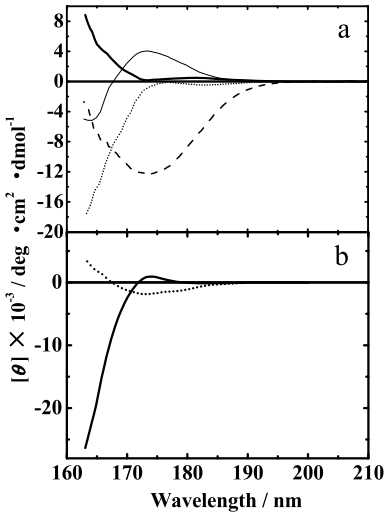

Fig. 2. Experimentally observed VUV-ECD spectra of methyl aldopyranosides in aqueous solution. (a) Methyl β-D-Glc (*thick solid line*), methyl α-D-Gal (*dotted line*), methyl β-D-Gal (*dashed line*) and methyl α-D-Glc (*thin solid line*) [18]. (b) Methyl α-D-Xyl (*solid line*) and methyl β-D-Xyl (*dotted line*). The spectra were recorded with a 1.0-mm slit width, an 8-s time constant, an 8-nm/min scan speed, and using four accumulations.

small positive peak around 181 nm and a large positive intensity at 163 nm, which differed markedly from the spectrum of methyl α-D-Glc exhibiting a positive peak around 172 nm and a negative peak around 163 nm. Methyl α-D-Gal showed a small negative peak around 183 nm and a large negative intensity at 163 nm, which were reversed in the spectrum of methyl β-D-Glc. Methyl β-D-Gal exhibited a negative peak around 174 nm that differed markedly from the spectrum of methyl α-D-Gal. Methyl α-D-Xyl and methyl β-D-Xyl showed a small negative and a positive peak around 175 nm, respectively, inverting their ECD signs below about 167 nm (Fig. 2(b)). These differences in spectra indicate that the VUV-ECD is very sensitive to the configurations of hydroxy groups at C-1 and C-4. These spectra for methyl aldopyranosides in heavy water were very close to those measured in water by Nelson and Johnson [23]. On the other hand, the spectra in film measured by Arndt and Stevens [1] differed markedly from those measured in water or heavy water, although the inversion of the spectra between methyl β-D-Glc and methyl α-D-Gal was conserved in film. These spectral differences would probably be due to differences in the populations of the GG, GT and TG rotamers [4,17,22,23] and/or differences in the electronic states of chromophores in the solution and solid states. These results mean that the solvent water must be considered when calculating the structures and VUV-ECD spectra of aldopyranosides in solution.

3.2. MD simulations of methyl aldopyranosides in a water bath

The structures of rotamers of methyl β-D-Glc, methyl α-D-Gal and methyl β-D-Gal were simulated in a water bath for 20 ns using AMBER 11. The dihedral angles of O-5–C-5–C-6–O-6 (60° for GT, −60° for GG and 180° for TG) were slightly restricted by the "RESTRAINTMASK" command [6,18]. The molecular parameters of the simulated GT, GG and TG rotamers of each methyl aldopyranoside are listed in Table 1. The bond lengths and bond angles of these three rotamers are almost invariant in the simulated structures of the three methyl aldopyranosides, but the dihedral angles differ markedly

Table 1
Bond lengths, bond angles and dihedral angles of the simulated structures of the GT, GG and TG rotamers

	Methyl β-D-Glc			Methyl α-D-Gal			Methyl β-D-Gal		
	GT	GG	TG	GT	GG	TG	GT	GG	TG
				Bond length (Å)					
O-5–C-5	1.371	1.509	1.415	1.457	1.550	1.504	1.456	1.398	1.468
C-1–O-5	1.438	1.499	1.368	1.459	1.464	1.490	1.515	1.485	1.447
O-1–C-1	1.437	1.465	1.467	1.465	1.459	1.476	1.534	1.452	1.517
C-6–C-5	1.538	1.567	1.514	1.527	1.515	1.505	1.524	1.540	1.512
C-3–C-4	1.490	1.525	1.527	1.520	1.487	1.531	1.575	1.538	1.528
C-7–O-1	1.433	1.427	1.410	1.477	1.484	1.479	1.473	1.478	1.507
				Bond angle (deg)					
C-1–O-5–C-5	116.830	112.650	119.890	117.000	114.620	116.510	110.440	120.900	115.160
O-1–C-1–O-5	108.146	104.909	107.643	112.258	113.153	107.301	109.110	110.150	110.891
C-7–O-1–C-1	112.160	118.380	114.340	118.360	113.600	123.200	113.920	113.790	109.580
O-5–C-5–C-4	107.910	106.800	109.470	110.950	102.930	108.550	111.710	106.280	110.710
O-5–C-5–C-6	105.260	106.490	112.600	105.130	114.150	106.460	103.530	102.580	102.820
HO-6–O-6–C-6	96.730	109.270	105.570	101.510	111.000	106.960	111.60	105.940	105.540
C-1–C-2–C-3	110.380	112.061	107.813	111.262	116.353	112.474	105.717	115.813	118.8534
				Dihedral angle (deg)					
C-7–O-1–C-1–O-5	−78.589	−61.875	−125.556	69.422	83.302	76.378	53.687	−78.977	−67.066
HO-2–O-2–C-2–C-1	174.040	150.702	85.306	−178.586	−46.100	−24.585	174.003	−65.540	−173.510
HO-4–O-4–C-4–C-3	80.273	70.225	16.274	−84.236	175.138	−48.907	86.068	133.695	−40.610
C-1–O-5–C-5–C-4	52.730	62.410	56.700	47.350	70.360	52.630	61.050	55.680	67.550
O-5–C-5–C-4–C-3	−57.380	−53.130	−49.690	−44.490	−63.990	−62.860	−59.790	−60.830	−54.390
C-5–C-4–C-3–C-2	59.680	49.970	53.740	51.890	57.726	62.650	53.890	57.048	43.349
O-5–C-5–C-6–O-6	54.150	−48.630	152.550	42.940	−47.850	153.260	59.450	−48.670	173.450
HO-6–O-6–C-6–C-5	−56.390	37.770	59.050	−35.880	63.030	−73.140	−47.410	79.810	−63.510

in the methoxy group (C-7–O-1–C-1–O-5), hydroxymethyl group (O-5–C-5–C-6–O-6) and hydroxy groups (e.g., HO-4–O-4–C-4–C-3). The fluctuations of these groups should affect the ECD spectra of aldopyranosides in solution, as we discussed previously [18].

3.3. ECD spectra of simulated structures of methyl aldopyranosides

Figure 3 shows the average ECD spectra calculated using the TDDFT method at the CAM-B3LYP/6-311++G** level for the 40 simulated structures of the GT, GG and TG rotamers of methyl β-D-Glc, methyl α-D-Gal and methyl β-D-Gal. The hydrated water molecules around methyl aldopyranosides were ignored in these calculations. Figure 3 also includes the theoretical ECD spectra for these three methyl aldopyranosides, which were estimated by a linear combination of the GT, GG and TG spectra based on their population ratios (GT : GG : TG = 47 : 50 : 3 in methyl β-D-Glc, 21 : 61 : 18 in methyl α-D-Gal and 22 : 55 : 23 in methyl β-D-Gal) [24].

The GT rotamer in methyl β-D-Glc (Fig. 3(a)) exhibited a negative peak around 173 nm and a positive peak around 160 nm, while the GG spectrum showed two successive positive peaks around 170 and 160 nm. The TG spectrum was similar to the GT spectrum except for a large difference in intensity below 160 nm. The differences in spectra among the rotamers demonstrate that ECD spectra are greatly

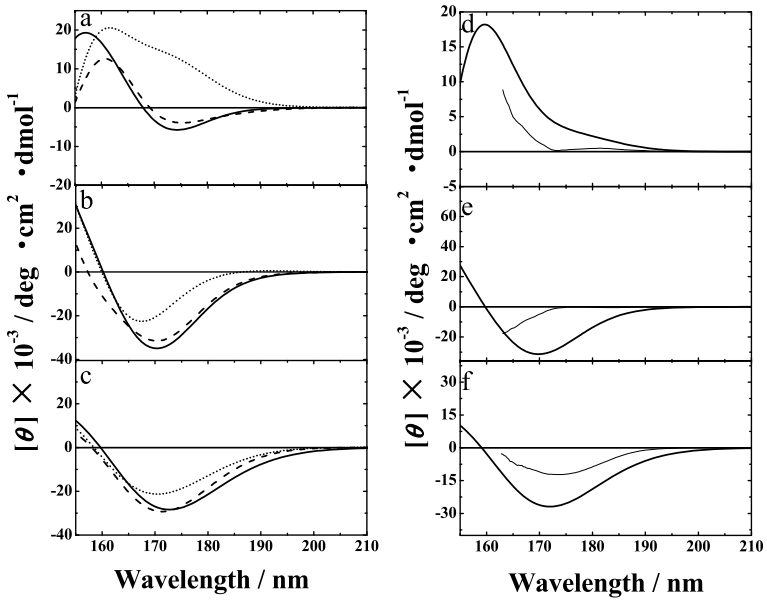

Fig. 3. Theoretical ECD spectra of the GT (*solid lines*), GG (*dotted lines*) and TG (*dashed lines*) rotamers of (a) methyl β-D-Glc, (b) methyl α-D-Gal and (c) methyl β-D-Gal calculated using the TDDFT method at the CAM-B3LYP/6-311++G** level. Each spectrum is the average of 40 spectra for the structures simulated at 500-ps intervals for 20 ns using AMBER 11. Theoretical ECD spectra (*thick solid lines*) of (d) methyl β-D-Glc, (e) methyl α-D-Gal and (f) methyl β-D-Gal, as estimated by a linear combination of the GT, GG and TG spectra based on their population ratios (GT : GG : TG = 47 : 50 : 3 in methyl β-D-Glc, 21 : 61 : 18 in methyl α-D-Gal and 22 : 55 : 23 in methyl β-D-Gal) [24]. Experimental spectra (*thin solid lines*) are included in (d), (e) and (f) for comparison.

affected by the conformations of the hydroxymethyl group at C-5 in methyl β-D-Glc. The three rotamers of methyl α-D-Gal commonly exhibited a negative peak around 170 nm, although the intensity around 170 nm was small for the GG spectrum compared to the other two rotamers (Fig. 3(b)). Similar spectra were also observed for three rotamers of methyl β-D-Gal (Fig. 3(c)), but the peaks around 170 nm for these rotamers were slightly red-shifted (by 2 or 3 nm) compared to those of the corresponding rotamers of methyl α-D-Gal.

The theoretically calculated spectrum of methyl β-D-Glc showed a positive peak around 160 nm accompanied by a small positive shoulder around 180 nm, as shown in Fig. 3(d). This theoretical spectrum resembles the experimental one: the shoulder around 180 nm is observed as a small positive peak around 181 nm, and the positive peak around 160 nm is expected to be observed below 163 nm. The theoretical spectrum of methyl α-D-Gal showed a negative peak around 170 nm (Fig. 3(e)), which differs markedly from the experimental one. On the other hand, the theoretical spectrum of methyl β-D-Gal reproduced the negative peak around 172 nm, although with a considerably different intensity (Fig. 3(f)). The negative peak around 172 nm for methyl β-D-Gal was slightly blue-shifted to 170 nm for methyl α-D-Gal in the theoretical calculation, whereas experiment suggests a large blue shift to a wavelength below 163 nm, which was the lower limit of the ECD measurements in this study. Although there are some limitations in the theoretical calculations, these results indicate that the conformations of methyl aldopyranosides obtained by MD simulations are suitable for calculating their ECD spectra, allowing the assignment of spectra obtained in TDDFT calculations of the molecular orbitals and rotational strengths.

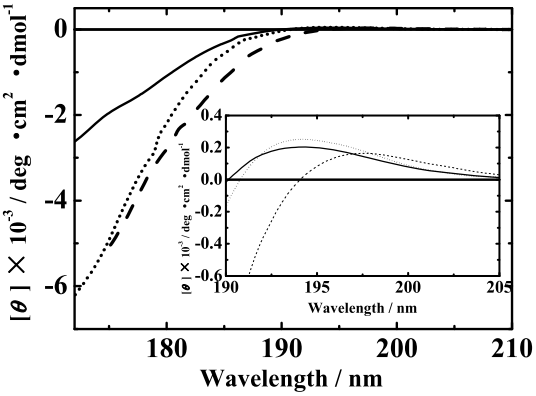

Fig. 4. VUV-ECD spectra of sorbitol (*solid line*), mannitol (*dashed line*) and arabitol (*dotted line*). Inset shows the expanded spectra in the wavelength region above 190 nm. The data acquisitions were the same as those for Fig. 2.

3.4. Assignments of VUV-ECD spectra of methyl aldopyranosides

The VUV-ECD spectra of methyl aldopyranosides were assigned based on the molecular orbitals and rotational strengths of the electronic transitions of hydroxy group, ring oxygen and methoxy oxygen, which were calculated using the TDDFT method at the CAM-B3LYP/6-311++G** level. The ECD in the wavelength region of 180–170 nm was mainly assigned to the n–σ^* transitions from the lone-pair orbital (n-orbital) to the σ^*-orbital of ring oxygen and methoxy oxygen, with only small contributions from hydroxy groups. The effects of these chromophores extended to the wavelength region below 170 nm. These assignments were essentially consistent with the results of Nelson and Johnson [23], Bertucci et al. [4], and our previous study of methyl α-D-Glc [18]. On the other hand, it is difficult to estimate the effects of hydroxy groups on the VUV-ECD spectra because the configuration of a hydroxy group might be affected not only by its own electronic transitions but also by those of ring oxygen and other oxygen atoms. Therefore, to determine the intrinsic effects of hydroxy groups on the VUV-ECD spectrum, we measured the VUV-ECD spectra of three polyols (sorbitol, mannitol and arabitol) that contain the hydroxy group only as a chromophore. As shown in Fig. 4, all of these polyols exhibited a very small positive peak around 195 nm and a large negative ECD around 170 nm, suggesting that the hydroxy groups contribute to ECD spectra only slightly around 195 nm but markedly around 170 nm. The hydroxy groups would therefore contribute to the ECD spectra of methyl aldopyranosides as described above.

3.5. Contributions of rotamers and anomers to ECD spectra

We recently reported that the theoretical GT and GG spectra of methyl α-D-Glc exhibit negative and positive ECD around 170 nm [18], respectively. As shown in Fig. 3(a), the GT and GG spectra of methyl β-D-Glc also exhibited negative and positive ECD around 170 nm. Further, all rotamers of methyl α-D-Gal (Fig. 3(b)) and methyl β-D-Gal (Fig. 3(c)) showed negative ECD around 170 nm, with the intensity being smaller for the GG rotamer than for the GT rotamer, implying that the GG conformation induces a positive ECD opposite to the GT rotamer in methyl α-D-Gal and methyl β-D-Gal. These results confirm that the GT and GG conformations cause negative and positive ECD around 170 nm, respectively, in all of the methyl aldopyranosides studied. The intensities of the ECD spectra of methyl α- and β-D-

Xyl with no hydroxymethyl group at C-5 were greatly reduced around 170 nm (Fig. 2(b)), which also represents evidence of the contributions of the rotamers in this wavelength region.

The experimental spectra of methyl α-D-Glc and methyl β-D-Glc showed negative and positive ECD around 163 nm, respectively (Fig. 2). Further, methyl α-D-Gal and methyl β-D-Gal exhibited negative ECD around 163 nm, with the intensity being smaller for the latter. These results suggest that the α- and β-anomers contribute negatively and positively to the ECD around 160 nm, respectively. This prediction is supported by the finding that methyl α-D-Xyl and methyl β-D-Xyl have negative and positive ECD around 163 nm, respectively (Fig. 2(b)).

3.6. Structural differences among GT, GG and TG rotamers

As described above, the theoretically calculated spectra of GT, GG and TG rotamers exhibited characteristic ECD in each methyl aldopyranoside (Fig. 3). The differences in the spectra among the GT, GG and TG rotamers would be mainly induced by changes in the molecular orbitals and rotational strengths of the ring oxygen (O-5) (see Section 3.4), which depend on the dihedral angle of the hydroxymethyl group of O-5–C-5–C-6–O-6 (+60°, −60° or 180°). To reveal the steric configuration between the hydroxymethyl group and the ring oxygen, the dihedral angle of HO-6–O-6–C-6–C-5 was plotted versus the distance between HO-6 and O-5 atoms in the GT, GG and TG rotamers of the three methyl aldopyranosides, as shown in Fig. 5. In all of the methyl aldopyranosides, the dihedral angles of HO-6–O-6–C-6–C-5 were around −50° and 50° for the GT and GG rotamers, respectively, within the interatomic distance of 2.4 Å, where the hydrogen atom (HO-6) could form a hydrogen bond to the ring oxygen (O-5) in both rotamers [18,21,32]. This hydrogen bond was retained for 10–13 ns of the total simulation

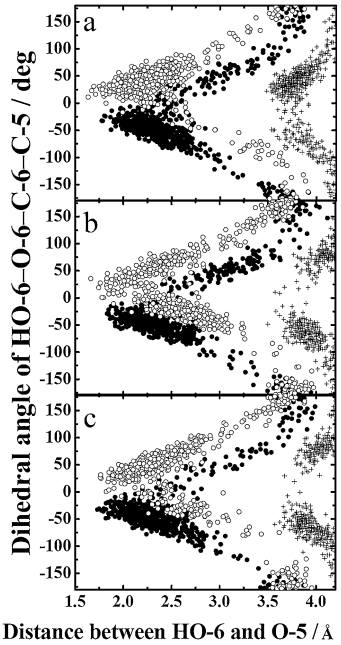

Fig. 5. Plots of dihedral angles of HO-6–O-6–C-6–C-5 versus the distance between HO-6 and O-5 atoms in the GT (*filled circles*), GG (*open circles*) and TG (*plus signs*) rotamers for (a) methyl β-D-Glc, (b) methyl α-D-Gal and (c) methyl β-D-Gal. The structure of each rotamer was simulated for 20 ns using AMBER 11.

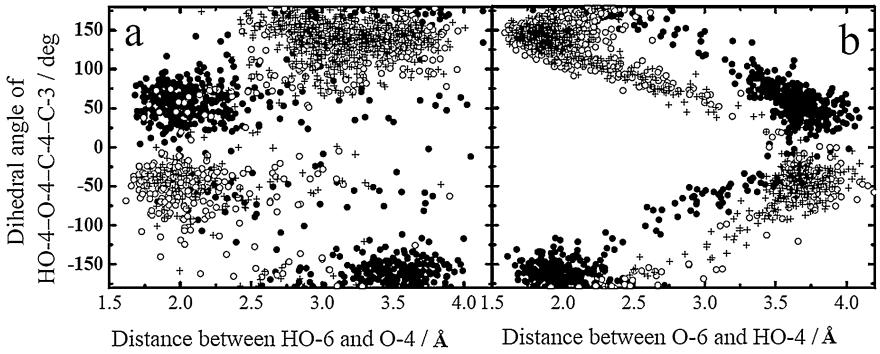

Fig. 6. Plots of dihedral angles of HO-4–O-4–C-4–C-3 versus (a) the distance between HO-6 and O-4 atoms and (b) the distance between O-6 and HO-4 atoms in the TG rotamer of methyl β-D-Glc (*filled circles*) and in the GG rotamers of methyl α-D-Gal (*open circles*) and methyl β-D-Gal (*plus signs*).

time (20 ns). On the other hand, the TG rotamers of the three methyl aldopyranosides showed no converged dihedral angle within the interatomic distance of 2.4 Å, meaning that no hydrogen bond can be formed between HO-6 and O-5 atoms in those rotamers (Fig. 5).

To clarify the steric configuration between the hydroxymethyl group and C-4 hydroxy group in the TG rotamer of methyl β-D-Glc and in the GG rotamers of methyl α-D-Gal and methyl β-D-Gal, we plotted the dihedral angle of HO-4–O-4–C-4–C-3 versus the distance between HO-6 and O-4 and the distance between O-6 and HO-4 (Fig. 6). In the TG rotamer of methyl β-D-Glc, the dihedral angle of HO-4–O-4–C-4–C-3 converged to about 50° within the distance of 2.4 Å between HO-6 and O-4 atoms (Fig. 6(a)), and to about −150° within the distance of 2.4 Å between O-6 and HO-4 atoms (Fig. 6(b)), implying the formations of two types of hydrogen bonds (O-6–HO-4 and O-4–HO-6). Either of these two hydrogen bonds was retained for about 18 ns (8 ns for O-4–HO-6 and 10 ns for O-6–HO-4). In the GG rotamers of methyl α-D-Gal and methyl β-D-Gal, the dihedral angle of HO-4–O-4–C-4–C-3 converged to about −50° within the distance of 2.4 Å between HO-6 and O-4 atoms (Fig. 6(a)), and to about 150° within the distance of 2.4 Å between O-6 and HO-4 atoms (Fig. 6(b)), indicating that two types of hydrogen bonds (O-4–HO-6 and O-6–HO-4) can be formed. Either of these two hydrogen bonds was maintained for about 18 ns (5 ns for O-4–HO-6 and 13 ns for O-6–HO-4). These localizations of the dihedral angle of HO-4–O-4–C-4–C-3 were not obtained in the GT and GG rotamers of methyl β-D-Glc, or in the GT and TG rotamers of methyl α-D-Gal and methyl β-D-Gal.

Based on these results, we speculated the steric configurations around the ring oxygen of the GT, GG and TG rotamers in the three methyl aldopyranosides, as shown in Fig. 7. In methyl β-D-Glc (Fig. 7(a)), the GT and GG rotamers form a hydrogen bond with different geometries between O-5 and HO-6 atoms. On the other hand, the TG rotamer forms two types of hydrogen bonds: O-6–HO-4 and O-4–HO-6. These configurations were basically the same as those speculated for methyl α-D-Glc [18]. The GT and GG rotamers of methyl α- and β-D-Gal keep a hydrogen bond between O-5 and HO-6 atoms, and further the GG rotamer exhibits an additional two types of hydrogen bonds between O-6 and HO-4 and between O-4 and HO-6 atoms (Fig. 7(b)). The hydroxymethyl group of TG rotamer in methyl α- and β-D-Gal has no hydrogen bond with either of O-5 or the hydroxy group at C-4. The steric configurations involving the hydroxy groups at C-2 and C-3, the methoxy group at C-1, and the sugar ring were similar among the GT, GG and TG rotamers in all of the methyl aldopyranosides (data not shown). Therefore, the different ECD spectra among these three rotamers at a given anomeric form could be dominantly ascribed to

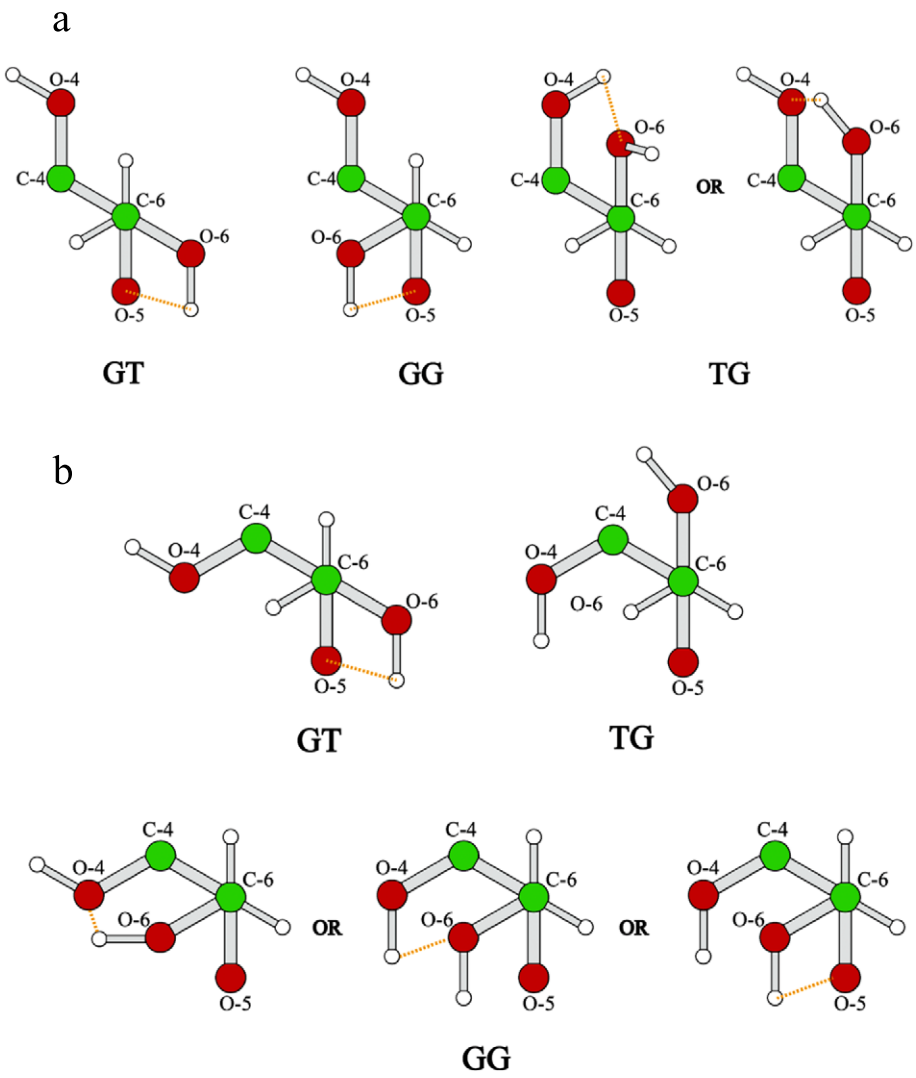

Fig. 7. Speculative steric configurations around the ring oxygen and the hydroxymethyl group of the GT, GG and TG rotamers (a) in methyl β-D-Glc and (b) in methyl α-D-Gal and methyl β-D-Gal in aqueous solution. Oxygen, hydrogen and carbon atoms are colored red, white and green, respectively. Yellow dotted lines indicate hydrogen bonds. The view in each panel is looking down the bond from C-6 to C-5. (The colors are visible in the online version of the article; http://dx.doi.org/10.3233/BSI-150116.)

the steric configurations including the hydrogen bonds around the C-5 hydroxymethyl group, the ring oxygen, and the C-4 hydroxy group.

3.7. Structural differences between α- and β-anomers

The theoretically calculated spectra of methyl aldopyranosides also exhibited the characteristic ECD dependence on the α- and β-anomers. These spectral characteristics of two anomers would be mainly induced by changes in the molecular orbitals and rotational strengths of O-1 methoxy oxygen (see Section 3.4). To clarify the structural differences between α- and β-anomers, the dihedral angles of the

hydroxy group of HO-2–O-2–C-2–C-1 were plotted versus the distance between HO-2 and O-1 atoms for three rotamers of methyl α-D-Gal and methyl β-D-Gal, as shown in Fig. 8. It is evident from the figure that the dihedral angles of HO-2–O-2–C-2–C-2 in all three rotamers were around $-50°$ for the α-anomer and around 50° for the β-anomer, within the interatomic distance of 2.4 Å, where the hydrogen atom (HO-2) could form a hydrogen bond with the methoxy oxygen (O-1). The retention time of this hydrogen bond was about 8 ns of the total simulation time (20 ns) in the α-anomer, while it was only 1–2 ns in the β-anomer. These different localizations in the dihedral angle of HO-2–O-2–C-2–C-2 were also observed in methyl α-D-Glc and methyl β-D-Glc.

Based on the above-described results, we speculate that the steric configurations around the methoxy oxygen of methyl aldopyranosides are as shown in Fig. 9. The α- and β-anomers should form a hydrogen bond between the O-1 and HO-2 atoms in the symmetrical configurations, although the hydrogen bond would be considerably more unstable in the β-anomer than in the α-anomer. The steric configurations involving the hydroxy groups at C-6, C-4 and C-3, and the sugar ring were similar between methyl α- and β-D-Glc or between methyl α- and β-D-Gal at a given rotamer conformation (data not shown), and so the difference between the ECD spectra for the α- and β-anomers in methyl aldopyranosides would be mainly due to the difference in the configurations including the hydrogen bonds related to the C-2 hydroxy group and the C-1 methoxy group.

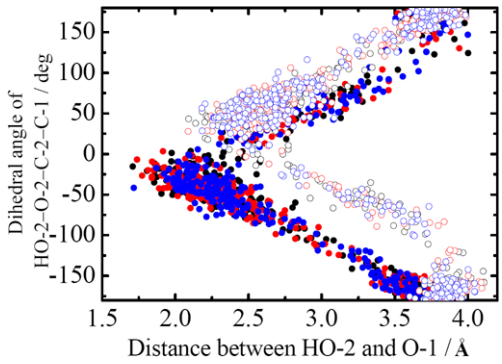

Fig. 8. Plots of dihedral angles of HO-2–O-2–C-2–C-1 versus the distances between HO-2 and O-1 atoms in the GT (black), GG (red) and TG (blue) rotamers for methyl α-D-Gal (*filled circles*) and methyl β-D-Gal (*open circles*). (The colors are visible in the online version of the article; http://dx.doi.org/10.3233/BSI-150116.)

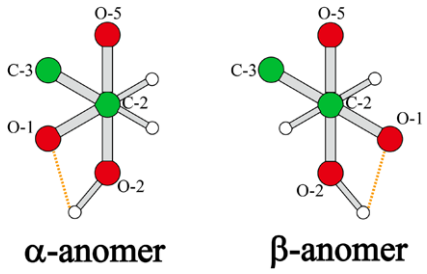

Fig. 9. Speculative steric configurations around the methoxy oxygen (*left*) of methyl α-D-Gal and methyl α-D-Glc and (*right*) of methyl β-D-Gal and methyl β-D-Glc in aqueous solution. Oxygen, hydrogen and carbon atoms are colored red, white and green, respectively. Yellow dotted lines indicate hydrogen bonds. The view in each panel is looking down the bond from C-2 to C-1. (The colors are visible in the online version of the article; http://dx.doi.org/10.3233/BSI-150116.)

4. Conclusions

It is difficult to determine the steric structures of saccharides using X-ray and NMR spectroscopy. However, in the present study, VUV-ECD spectroscopy combined with TDDFT and MD methods revealed some pairwise relationships between the steric configurations and ECD spectra of monosaccharides, demonstrating that this spectroscopy is a useful tool for determining the complicated equilibrium structures of saccharides in aqueous solution, although there are some limitations. Further advanced VUV-ECD spectroscopy coupled with theoretical calculations could be practicable for analyzing the structural changes in saccharides induced by interactions with biomolecules such as proteins and cell membranes, and would open new fields in the molecular sciences of glycoconjugates.

Acknowledgements

This work was supported by JSPS Research Fellowship for Young Scientists (K.M.) (nos. 19001913 and 23687020) and by a grant from Kurata Memorial Hitachi Science and Technology Foundation.

References

[1] E.R. Arndt and E.S. Stevens, Vacuum ultraviolet circular dichroism studies of simple saccharides, *J. Am. Chem. Soc.* **115** (1993), 7849–7853.
[2] H.J.C. Berendsen, J.P.M. Postma, W.F. van Gunsteren, A. DiNola and J.R. Haak, Molecular dynamics with coupling to an external bath, *J. Chem. Phys.* **81** (1984), 3684–3690.
[3] N. Berova, K. Nakanishi and R.W. Woody, *Circular Dichroism: Principles and Applications*, 2nd edn, John Wiley & Sons, New York, 2000.
[4] C. Bertucci, P. Salvadori, Z. Giampaolo, D. Pini and W.C. Johnson Jr., Circular dichroism spectra of some model compounds related to D-glucopyranose and D-galactopyranose, *Carbohydr. Chem.* **149** (1986), 299–307.
[5] D.A. Case, T.A. Darden, T.E. Cheatham, C.L. Simmerling, J. Wang, R.E. Duke, R. Luo, R.C. Walker, W. Zhang, K.M. Merz et al., AMBER 11, University of California, San Francisco, 2010.
[6] J.R. Cheeseman, M.S. Shaik, P.L.A. Popelier and E.W. Blanch, Calculation of Raman optical activity spectra of methyl-β-D-glucose incorporating a full molecular dynamics simulation of hydration effects, *J. Am. Chem. Soc.* **133** (2011), 4991–4997.
[7] T. Darden, D. York and L. Pedersen, Particle mesh Ewald: An $N \cdot \log(N)$ method for Ewald sums in large systems, *J. Chem. Phys.* **98** (1993), 10089–10092.
[8] G.D. Fasman, *Circular Dichroism and the Conformational Analysis of Biomolecules*, Plenum Press, New York, 1996.
[9] T. Fukuyama, K. Matsuo and K. Gekko, Vacuum-ultraviolet electronic circular dichroism of L-alanine in aqueous solution investigated by time-dependent density functional theory, *J. Phys. Chem. A* **109** (2005), 6928–6933.
[10] T. Fukuyama, K. Matsuo and K. Gekko, Experimental and theoretical studies of vacuum-ultraviolet electronic circular dichroism of hydroxy acids in aqueous solution, *Chirality* **23** (2011), E52–E58.
[11] G.B. Jagdale, P.S. Grewal and S. Salminen, Both heat-shock and cold-shock influence trehalose metabolism in an entomopathogenic nematode, *J. Parasitol.* **91** (2005), 988–994.
[12] W.C. Johnson Jr., The circular dichroism of carbohydrates, *Adv. Carbohydr. Chem. Biochem.* **45** (1986), 73–124.
[13] W.L. Jorgensen and C. Jenson, Temperature dependence of TIP3P, SPC, and TIP4P water from NPT Monte Carlo simulations: Seeking temperatures of maximum density, *J. Comput. Chem.* **19** (1998), 1179–1186.
[14] K.N. Kirschner and R.J. Woods, Solvent interactions determine carbohydrate conformation, *Proc. Natl. Acad. Sci. USA* **98** (2001), 10541–10545.
[15] K.N. Kirschner, A.B. Yongye, S.M. Tschampel, J. González-Outeiriño, C.R. Daniels, B.L. Foley and R.J. Woods, GLYCAM06: A generalizable biomolecular force field. Carbohydrates, *J. Comput. Chem.* **29** (2008), 622–655.
[16] M.N.V.R. Kumar, A review of chitin and chitosan applications, *React. Func. Polym.* **46** (2000), 1–27.
[17] K. Matsuo and K. Gekko, Vacuum-ultraviolet circular dichroism study of saccharides by synchrotron radiation spectrophotometry, *Carbohydr. Res.* **339** (2004), 591–597.

[18] K. Matsuo, H. Namatame, M. Taniguchi and K. Gekko, Vacuum-ultraviolet electronic circular dichroism study of methyl α-D-glucopyranoside in aqueous solution by time-dependent density functional theory, *J. Phys. Chem. A* **40** (2012), 9996–10003.
[19] K. Matsuo, K. Sakai, Y. Matsushima, T. Fukuyama and K. Gekko, Optical cell with a temperature-control unit for a vacuum-ultraviolet circular dichroism spectrophotometer, *Anal. Sci.* **19** (2003), 129–132.
[20] S. Miertus, E. Scrocco and J. Tomasi, Electrostatic interaction of a solute with a continuum. A direct utilization of *Ab initio* molecular potentials for the prevision of solvent effects, *Chem. Phys.* **55** (1981), 117–129.
[21] C. Molteni and M. Parrinello, Glucose in aqueous solution by first principles molecular dynamics, *J. Am. Chem. Soc.* **120** (1998), 2168–2171.
[22] R.G. Nelson and W.C. Johnson Jr., Optical properties of sugars. I. Circular dichroism of monomers at equilibrium, *J. Am. Chem. Soc.* **94** (1972), 3343–3345.
[23] R.G. Nelson and W.C. Johnson Jr., Optical properties of sugars. 4. Circular dichroism of methyl aldopyranosides, *J. Am. Chem. Soc.* **98** (1976), 4296–4301.
[24] Y. Nishida, H. Hori, H. Ohrui and H. Meguro, ^{1}H NMR analyses of rotameric distribution of C5–C6 bonds of D-glucopyranoses in solution, *J. Carbohydr. Chem.* **7** (1988), 239–250.
[25] N. Ojima, K. Sakai, K. Matsuo, T. Matsui, T. Fukazawa, H. Namatame, M. Taniguchi and K. Gekko, Vacuum-ultraviolet circular dichroism spectrophotometer using synchrotron radiation: Optical system and on-line performance, *Chem. Lett.* **30** (2001), 522–523.
[26] S. Pérez and M.-M. Delage, A database of three-dimensional structures of monosaccharides from molecular-mechanics calculations, *Carbohydr. Res.* **212** (1991), 253–259.
[27] A. Racaud, A.R. Allouche, R. Antoine, J. Lemoine and P. Dugourd, UV electronic excitations in acidic sugars, *J. Mol. Struct.: THEOCHEM* **960** (2010), 51–56.
[28] J.-P. Ryckaert, G. Ciccotti and H.J.C. Berendsen, Numerical integration of the Cartesian equations of motion of a system with constraints: Molecular dynamics of *n*-alkanes, *J. Comput. Phys.* **23** (1977), 327–341.
[29] M.A. Schneegurt, D.M. Sherman, S. Nayar and L.A. Sherman, Oscillating behavior of carbohydrate granule formation and dinitrogen fixation in the cyanobacterium *Cyanothece* sp. strain ATCC 51142, *J. Bacteriol.* **176** (1994), 1586–1597.
[30] N. Sharon and H. Lis, Lectins as cell recognition molecules, *Science* **246** (1989), 227–234.
[31] C. Simmerling, T. Fox and P.A. Kollman, Use of locally enhanced sampling in free energy calculations: Testing and application to the $\alpha \rightarrow \beta$ anomerization of glucose, *J. Am. Chem. Soc.* **120** (1998), 5771–5782.
[32] T. Suzuki, The hydration of glucose: The local configurations in sugar–water hydrogen bonds, *Phys. Chem. Chem. Phys.* **10** (2008), 96–105.
[33] T. Yanai, D.P. Tew and N.C.A. Handy, A new hybrid exchange–correlation functional using the Coulomb-attenuating method (CAM-B3LYP), *Chem. Phys. Lett.* **393** (2004), 51–57.